

2 **Simulation Studies for a High-Pressure Active-Target** 3 **TPC to Measure the Proton Charge Radius in** 4 **Muon-Proton Elastic Scattering**

5 **Martin Hoffmann,^a Fabian Metzger,^{a,b} and Bernhard Ketzer^{a,1}**

6 *^aHelmholtz-Institut für Strahlen- und Kernphysik, Universität Bonn,*
7 *Nussallee 14-16, D-53115 Bonn, Germany*

8 *^bEuropean Organization for Nuclear Research (CERN), 1211 Geneva 23,*
9 *Switzerland*

10 *E-mail: Bernhard.Ketzer@uni-bonn.de*

11 **ABSTRACT:** The AMBER collaboration plans to perform a measurement of the proton charge
12 radius using high-energy muon-proton elastic scattering. The energy transfer to the proton will
13 be measured with an active-target time projection chamber. This study shows simulations of the
14 readout segmentation of this detector, leading to the used layout for a pilot run in 2021.

15 **KEYWORDS:** Time Projection Chamber, TPC, Proton Charge Radius, Active Target

¹Corresponding author

16	Contents	
17	1 Introduction	1
18	2 Methods	1
19	2.1 Signal generation	1
20	2.2 Signal reconstruction	2
21	3 Results and conclusion	3

22 1 Introduction

23 Active-target Time Projection Chambers (TPCs) filled with hydrogen or helium gas are an extremely
24 powerful and at times the only way to reconstruct very low-energy recoil particles from interactions
25 of beam particles with the atoms of the detector medium, which acts as a target at the same time.
26 An active-target TPC without charge amplification will be the main device for the measurement
27 of the proton charge radius at the AMBER experiment at CERN SPS. The TPC will use hydrogen
28 gas at pressures of up to 20 bar. The challenge at the AMBER experiment is to reconstruct the
29 recoil proton in the background of a high-intensity wide muon beam. At values of the squared
30 momentum transfer of the order of $5 \cdot 10^{-4} \text{ GeV}^2/c^2$, the kinetic energy of the proton is only
31 $\sim 300 \text{ keV}$, corresponding to a range less than one cm. We perform detailed simulations of the
32 setup including beam-induced noise at different gas pressures in order to define the granularity of
33 the readout structure and optimize the energy and angular resolution.

34 2 Methods

35 In order to study the impact of different pad plane layouts, we perform simulations. This requires
36 both the signal generation and the signal reconstruction.

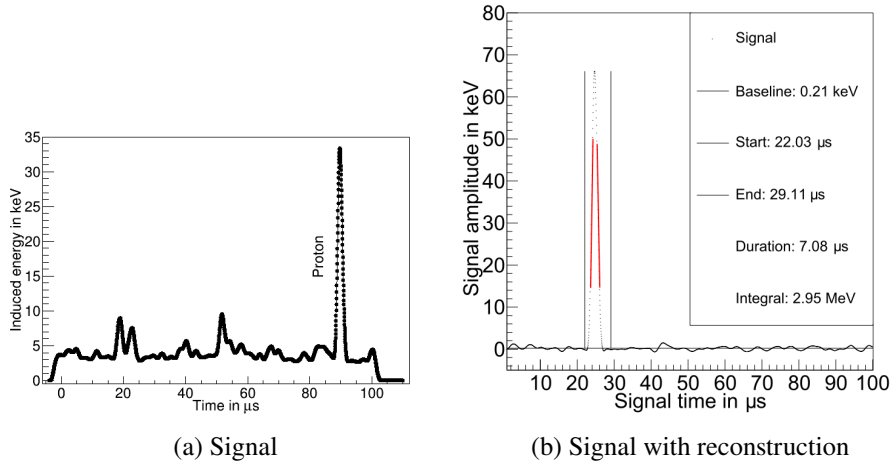
37 2.1 Signal generation

38 We use an existing TGEANT framework, which is based on GEANT4 to simulate the AMBER
39 setup. We have implemented the active-target TPC with all relevant elements in the simulation.
40 Starting with a 100 GeV muon beam, an elastic scattering process is triggered for the simulation.
41 The energy deposit in the TPC is simulated for the recoil proton as well as for beam particles
42 within a time window to create a constant background over the processed 100 μs signal. This
43 energy deposit is converted to drift electrons, which then are propagated to the readout using the
44 parameters listed in table 1. The induced signal of the drift electrons is simulated with pad response
45 functions calculated using GARFIELD++ with MAGBOLTZ[1].

Table 1: Drift and diffusion parameters [1].

Region	E in kV cm^{-1}	p in bar	v_{Drift} in cm ms^{-1}	\bar{D}_T in $\mu\text{m cm}^{-0.5}$	\bar{D}_L in $\mu\text{m cm}^{-0.5}$
Drift	0.464	4.0	417.1 ± 0.4	158.7 ± 2.2	125.5 ± 1.3
	2.32	20.0	417.0 ± 0.4	70.6 ± 0.8	57.6 ± 1.4
Induction	2.0	4.0	841.6 ± 0.7	131.6 ± 1.9	87.8 ± 1.6
	10.0	20.0	841.8 ± 0.7	58.7 ± 0.8	38.5 ± 0.8

46 Additionally, we simulate electronic noise according to measurements from a 2018 test mea-
 47 surement (from A. Dzyuba) before applying a shaping function originating from the electronics.
 48 The resulting signal can be seen in figure 1. The signal by the recoil proton is clearly visible above
 49 the background.

**Figure 1:** Simulated signals of the TPC.

50 2.2 Signal reconstruction

51 The signal visible in figure 1 can be integrated inside a time window given by extrapolations of
 52 the rising and trailing edge of the signal. For this integration, the baseline given by the constant
 53 background is subtracted.

54 We can sum up over the integrated signals with time and energy cuts to reconstruct the recoil
 55 proton track, see figure 2. If the recoil proton is contained within the TPC, the energy sum of all
 56 added pads gives the kinetic energy. This energy can then be compared to the simulated proton
 57 energy to study the uncertainty of the reconstruction. By performing a linear fit, we can also extract
 58 the azimuthal angle and compare to the simulations.

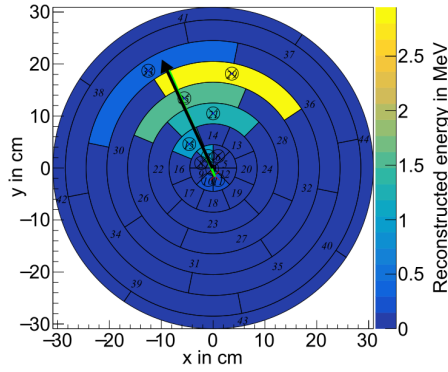


Figure 2: A simulated and reconstructed event in the TPC readout. The simulated Monte Carlo track is drawn in green with the vertex as red cross, the reconstructed track is given in black.

59 The reconstruction was compared to measured noise levels of the central pad of the ACTAF
 60 TPC in the MAMI-experiment (from 2018), see figure 3. The beam noise was simulated on different
 61 rings .

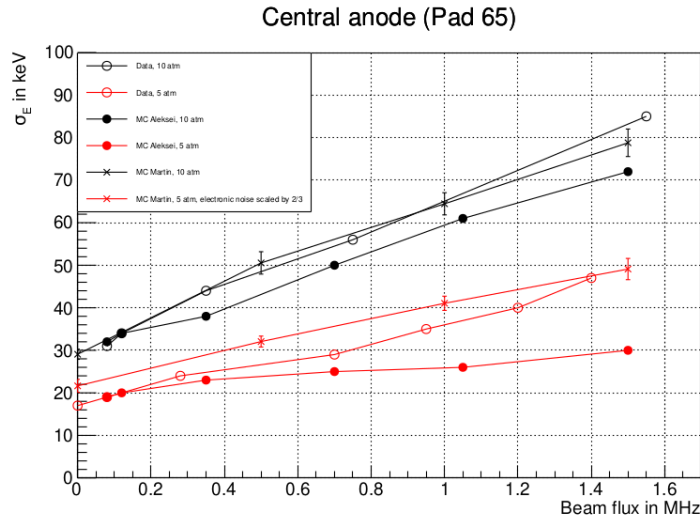


Figure 3: Simulation of combined noise for the central pad of the ACTAF TPC in the MAMI-experiment. The TPC was filled with 96 % He and 4 % N2.

62 3 Results and conclusion

63 The simulated energy resolution is similar for all compared pad planes, see figure 4. For the angular
 64 resolution, we see a large improvement by rotating the outer rings, see figure 5. Additionally, the
 65 pad planes with a higher segmentation on the second ("PRM2" or "PRM6") as well as the second
 66 and third ring ("PRM3" or "PRM7") show better resolutions.

67 With the help of these studies, we chose a pad plane for the pilot run 2021, see figure 6.
 68 The second ring has been segmented into 8 instead of 4 pads. Additionally, the outer rings have

69 been rotated to gain additional angular resolution, without having to further increase the number of
 70 readout channels and retaining the same energy resolution.

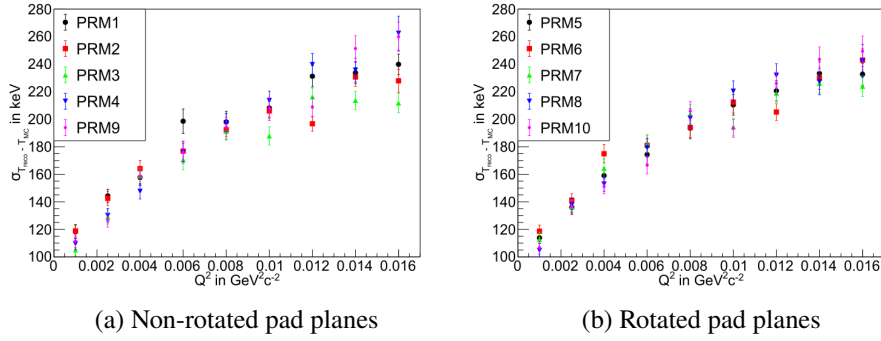


Figure 4: Resulting energy resolutions of the simulated pad planes. We see a similar resolution for all options.

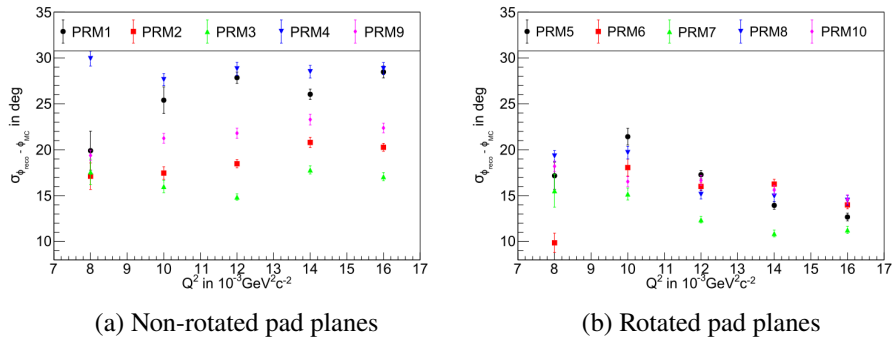


Figure 5: Resulting angular resolutions of the simulated pad planes. We see a much better resolution for the rotated pad planes. The pad planes with a higher segmentation on the second ("PRM2" or "PRM6") as well as the second and third ring ("PRM3" or "PRM7") improve the resolution further.

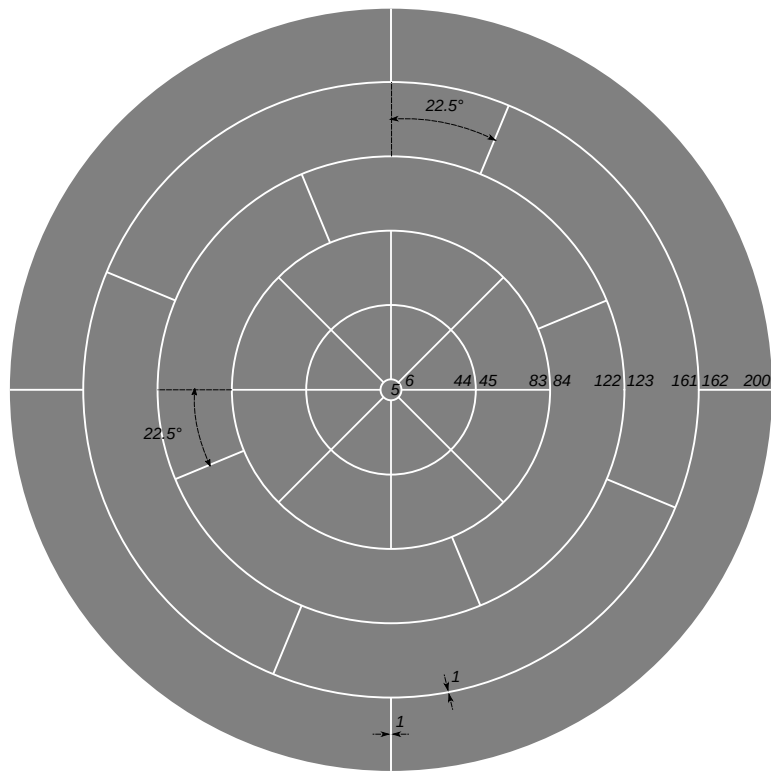


Figure 6: Optimized pad plane for the PRM pilot run 2021. The rotated readout improves the azimuthal precision, while keeping the same number of readout channels and energy resolution.

71 **Acknowledgments**

72 This activity is partially supported by EU Horizon 2020 research and innovation programme,
 73 STRONG-2020 project, under grant agreement no. 824093.

74 **References**

75 [1] F. Metzger, *Simulations of an active-target TPC for a measurement of the proton charge radius*,
 76 Master's thesis, Rheinische Friedrich-Wilhelms-Universität Bonn, 2020.